

# Something about $Z$ -penguins I want to tell

Ulrich Haisch

*Institut für Physik (THEP), Johannes Gutenberg-Universität, D-55099 Mainz, Germany*

We stress that in models with constrained minimal flavor violation large negative corrections to the flavor-changing  $Z$ -penguin amplitudes are excluded by the precision measurements of the  $Z \rightarrow b\bar{b}$  pseudo observables performed at LEP and SLC. The derived stringent range for the non-standard contribution to the universal Inami-Lim function  $C$  leads to tight two-sided limits for the branching ratios of all  $Z$ -penguin dominated flavor-changing  $K$ - and  $B$ -decays.

## 1. INTRODUCTION

The effects of new heavy particles appearing in extensions of the standard model (SM) can be accounted for at low energies in terms of effective operators. The unprecedented accuracy reached by the electroweak (EW) precision measurements performed at the high-energy colliders LEP and SLC impose stringent constraints on the coefficients of the operators entering the EW sector. Other severe constraints came in recent years from the BaBar, Belle, CDF, and  $D\bar{D}$  experiments and concern extra sources of flavor and CP violation that represent a generic problem in many beyond the SM (BSM) scenarios. The most pessimistic but experimentally well supported solution to the flavor puzzle is to assume that all flavor and CP violation is governed by the known structure of the SM Yukawa interactions. In these minimal flavor violating (MFV) [1, 2] models, correlations between certain flavor diagonal high-energy and flavor off-diagonal low-energy observables exist since, by construction, BSM physics couples dominantly to the third generation. To simplify matters, we restrict ourselves in the following to scenarios that involve only SM operators, so-called constrained MFV (CMFV) [3] models, and thus consider only left-handed currents. Correlations between flavor diagonal and off-diagonal amplitudes, similar to the ones discussed below, might exist in many beyond-MFV scenarios in which the modification of the flavor structure is non-universal. One example for such a correlation is provided by the intimate relation between the  $b \rightarrow sZ$  and  $Z \rightarrow b\bar{b}$  amplitude [4] present in the original Randall-Sundrum scenario [5].

## 2. GENERAL CONSIDERATIONS

That new interactions unique to the third generation can lead to a strong correlation between the non-universal  $Zb_L\bar{b}_L$  and the flavor non-diagonal  $Zd_L^j\bar{d}_L^i$  vertices has been shown in [6]. Whereas the former structure is probed by the ratio of the  $Z$ -boson decay width into bottom quarks and the total hadronic width,  $R_b^0$ , the bottom quark asymmetry parameter,  $\mathcal{A}_b$ , and the forward-backward asymmetry for bottom quarks,  $A_{FB}^{0,b}$ , the latter ones appear in many  $K$ - and  $B$ -decays.

In the effective field theory framework of MFV [2], it is easy to see how the  $Zb_L\bar{b}_L$  and  $Zd_L^j\bar{d}_L^i$  operators are linked together. The only relevant dimension-six contributions compatible with the flavor group of MFV stem from the  $SU(2) \times U(1)$  invariant operators

$$\mathcal{O}_1 = i \left( \bar{Q}_L Y_U Y_U^\dagger \gamma_\mu Q_L \right) \phi^\dagger D^\mu \phi, \quad \mathcal{O}_2 = i \left( \bar{Q}_L Y_U Y_U^\dagger \tau^a \gamma_\mu Q_L \right) \phi^\dagger \tau^a D^\mu \phi, \quad (1)$$

that are built out of the quark doublets  $Q_L$ , the Higgs field  $\phi$ , the up-type Yukawa matrices  $Y_U$ , and the  $SU(2)$  generators  $\tau^a$ . After EW symmetry breaking,  $\mathcal{O}_{1,2}$  are responsible for both the effective  $Zb_L\bar{b}_L$  and  $Zd_L^j\bar{d}_L^i$  vertex. Since all up-type quark Yukawa couplings except the one of the top,  $y_t$ , are small, one has  $(Y_U Y_U^\dagger)_{ji} \sim y_t^2 V_{tj}^* V_{ti}$  and only this contribution matters in Eq. (1).

Within the SM the Feynman diagrams responsible for the enhanced top correction to the  $Zb_L\bar{b}_L$  coupling also generate the  $Zd_L^j\bar{d}_L^i$  operators. In fact, in the limit of infinite top quark mass the corresponding amplitudes are up to

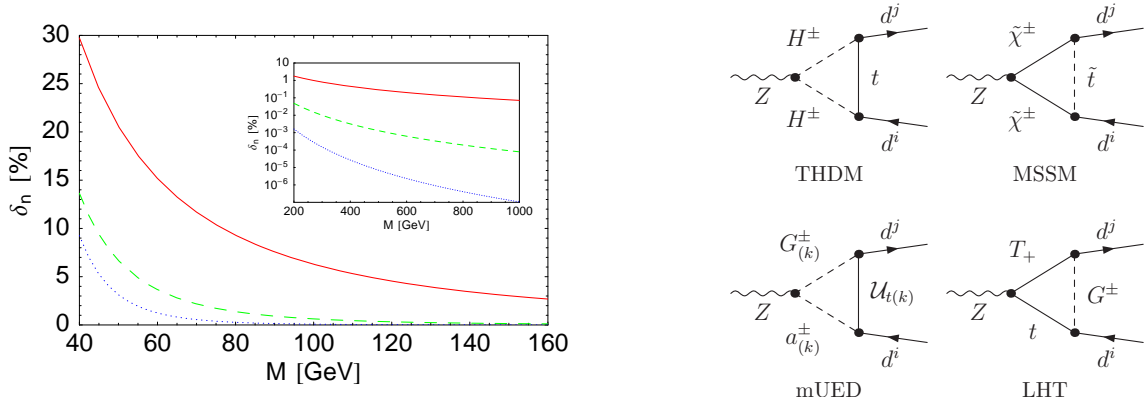


Figure 1: Left: Relative deviations  $\delta_n$  as a function of  $M$ . The solid, dashed, and dotted curve correspond to  $n = 1, 2$ , and  $3$ , respectively. Right: Examples of one-loop vertex diagrams that result in a non-universal correction to the  $Z \rightarrow d^j \bar{d}^i$  transition in assorted BSM scenarios with CMFV. See text for details.

Cabibbo-Kobayashi-Maskawa (CKM) factors identical. Yet there is an important difference between them. While for the physical  $Z \rightarrow b\bar{b}$  decay the diagrams are evaluated on-shell, in the case of the low-energy  $Z \rightarrow d^j \bar{d}^i$  transitions the amplitudes are Taylor-expanded up to zeroth order in the external momenta. As far as the momentum of the  $Z$ -boson is concerned the two cases correspond to  $q^2 = M_Z^2$  and  $q^2 = 0$ .

The general features of the small momentum expansion of the one-loop  $Z \rightarrow b\bar{b}$  vertex can be nicely illustrated with the following simple but educated example. Consider the scalar integral

$$C_0 = \frac{m_3^2}{i\pi^2} \int \frac{d^4 l}{D_1 D_2 D_3}, \quad D_i = (l + p_i)^2 - m_i^2, \quad (2)$$

with  $p_3 = 0$ . In the limit of vanishing bottom quark mass one has for the corresponding momenta  $p_1^2 = p_2^2 = 0$ . The small momentum expansion of the scalar integral  $C_0$  then takes the form

$$C_0 = \sum_{n=0}^{\infty} a_n \left( \frac{q^2}{m_3^2} \right)^n, \quad (3)$$

with  $q^2 = (p_1 - p_2)^2 = -2p_1 \cdot p_2$ . Analytic expressions for the expansion coefficients  $a_n$  have been given in [6]. Here we confine ourselves to the simplified case  $m_1 = m_2 = M$  and  $m_3 = m_t$ . We define

$$\delta_n = a_n \left( \frac{M_Z^2}{m_t^2} \right)^n \left( \sum_{l=0}^{n-1} a_l \left( \frac{M_Z^2}{m_t^2} \right)^l \right)^{-1}, \quad (4)$$

for  $n \geq 1$ . The  $M$ -dependence of the relative deviations  $\delta_n$  is displayed on the left in Fig. 1. We see that while for  $M \lesssim 50$  GeV higher order terms in the small momentum expansion have to be included in order to approximate the exact on-shell result accurately, in the case of  $M \gtrsim 150$  GeV the first correction is small and higher order terms are negligible. For the two reference scales  $M = \{80, 250\}$  GeV one finds for the first three relative deviations  $\delta_n$  numerically +9.3%, +1.4%, and +0.3%, and +1.1%, +0.02%, +0.00004%, respectively.

Of course the two reference points  $M = \{80, 250\}$  GeV have been picked for a reason. While the former describes the situation in the SM, *i.e.*, the exchange of two pseudo Goldstone bosons and a top quark, the latter presents a possible BSM contribution involving besides the top, two heavy scalars. The above example indicates that the differences between the  $Z b_L \bar{b}_L$  form factor evaluated on-shell and at zero external momenta are in general much less pronounced in models with new heavy degrees of freedom than in the SM. Given that this difference amounts to around  $-30\%$  in the SM, it is suggestive to assume that the scaling of BSM contributions to the non-universal  $Z b_L \bar{b}_L$  vertex is in general under  $\pm 10\%$ . This model-independent conclusion is well supported by the results of the calculations of the one-loop  $Z b_L \bar{b}_L$  vertices in popular CMFV models presented in [6].

### 3. MODEL CALCULATIONS

The above considerations can be corroborated in another, yet model-dependent way by explicitly calculating the difference between the value of the  $Z d_L^j \bar{d}_L^i$  vertex form factor evaluated on-shell and at zero external momenta. In [6] this has been done in four of the most popular, consistent, and phenomenologically viable scenarios of CMFV, *i.e.*, the two-Higgs-doublet model (THDM) type I and II, the minimal supersymmetric SM (MSSM) with MFV, all for small  $\tan\beta$ , the minimal universal extra dimension (mUED) model [7], and the littlest Higgs model [8] with  $T$ -parity (LHT) [9] and degenerate mirror fermions [10]. Examples of diagrams that contribute to the  $Z \rightarrow d^j \bar{d}^i$  transition in these models can be seen on the right of Fig. 1. In the following we will briefly summarize the most important findings of [6].

In the limit of vanishing bottom quark mass, possible non-universal BSM contributions to the renormalized off-shell  $Z d_L^j \bar{d}_L^i$  vertex can be written as

$$\Gamma_{ji}^{\text{BSM}} = \frac{G_F}{\sqrt{2}} \frac{e}{\pi^2} M_Z^2 \frac{c_w}{s_w} V_{tj}^* V_{ti} C_{\text{BSM}}(q^2) \bar{d}_L^j \gamma_\mu d_L^i Z^\mu, \quad (5)$$

where  $i = j = b$  and  $i \neq j$  in the flavor diagonal and off-diagonal case.  $G_F$ ,  $e$ ,  $s_w$ , and  $c_w$  denote the Fermi constant, the electromagnetic coupling constant, the sine and cosine of the weak mixing angle, respectively, while  $V_{ij}$  are the corresponding CKM matrix elements.

As a measure of the relative difference between the complex valued form factor  $C_{\text{BSM}}(q^2)$  evaluated on-shell and at zero momentum we introduce

$$\delta C_{\text{BSM}} = 1 - \frac{\text{Re } C_{\text{BSM}}(q^2 = 0)}{\text{Re } C_{\text{BSM}}(q^2 = M_Z^2)}. \quad (6)$$

The dependence of  $\delta C_{\text{BSM}}$  on the compactification scale  $1/R$  of the mUED model and  $x_L$ , which parametrizes the mass of the heavy top  $T_+$  in the LHT scenario, is illustrated in the two plots on the left-hand side in Fig. 2. The allowed parameter regions after applying the  $\bar{B} \rightarrow X_s \gamma$  constraint in the case of the mUED model [11] and electroweak precision measurements in the case of the LHT scenario [12] are indicated by the colored (grayish) bands.

In the THDMs, the mUED, and the CMFV version of the LHT model the maximal allowed suppressions of  $\text{Re } C_{\text{BSM}}(q^2 = M_Z^2)$  with respect to  $\text{Re } C_{\text{BSM}}(q^2 = 0)$  amounts to less than 2%, 5%, and 4%, respectively. This feature confirms the general argument presented in the last section. The situation is less favorable in the case of the CMFV MSSM, since  $\delta C_{\text{MSSM}}$  frequently turns out to be larger than one would expect on the basis of the model-independent considerations if the masses of the lighter chargino and stop both lie in the hundred GeV range. However, the large deviation  $\delta C_{\text{MSSM}}$  are ultimately no cause of concern, because  $|\text{Re } C_{\text{MSSM}}(q^2 = 0)/\text{Re } C_{\text{SM}}(q^2 = 0)|$  itself is always below 10%. In consequence, the model-independent bounds on the BSM contribution to the universal  $Z$ -penguin function that will be derived in the next section do hold in the case of the CMFV MSSM. More details on the phenomenological analysis of  $\delta C_{\text{BSM}}$  in the THDMs, the CMFV MSSM, the mUED, and the LHT model including the analytic expressions for the form factors  $C_{\text{BSM}}(q^2)$  can be found in [6].

### 4. NUMERICAL ANALYSIS

The BSM contribution  $\Delta C = \text{Re } C(q^2 = 0) - \text{Re } C_{\text{SM}}(q^2 = 0)$  can be extracted in a model-independent fashion from a global fit to the pseudo observables  $R_b^0$ ,  $\mathcal{A}_b$ , and  $A_{\text{FB}}^{0,b}$  and the measured  $\bar{B} \rightarrow X_s \gamma$  and  $\bar{B} \rightarrow X_s l^+ l^-$  branching ratios. Neglecting contributions from EW boxes these bounds read [6]

$$\Delta C = -0.026 \pm 0.264 \quad (68\% \text{ CL}), \quad \Delta C = [-0.483, 0.368] \quad (95\% \text{ CL}). \quad (7)$$

These numbers imply that large negative contributions that would reverse the sign of the SM  $Z$ -penguin amplitude are highly disfavored in CMFV scenarios due to the strong constraint from  $R_b^0$  [6]. Interestingly, such a conclusion cannot be drawn by considering only flavor constraints [13], since at present, a combination of  $\mathcal{B}(\bar{B} \rightarrow X_s \gamma)$ ,  $\mathcal{B}(\bar{B} \rightarrow X_s l^+ l^-)$ ,

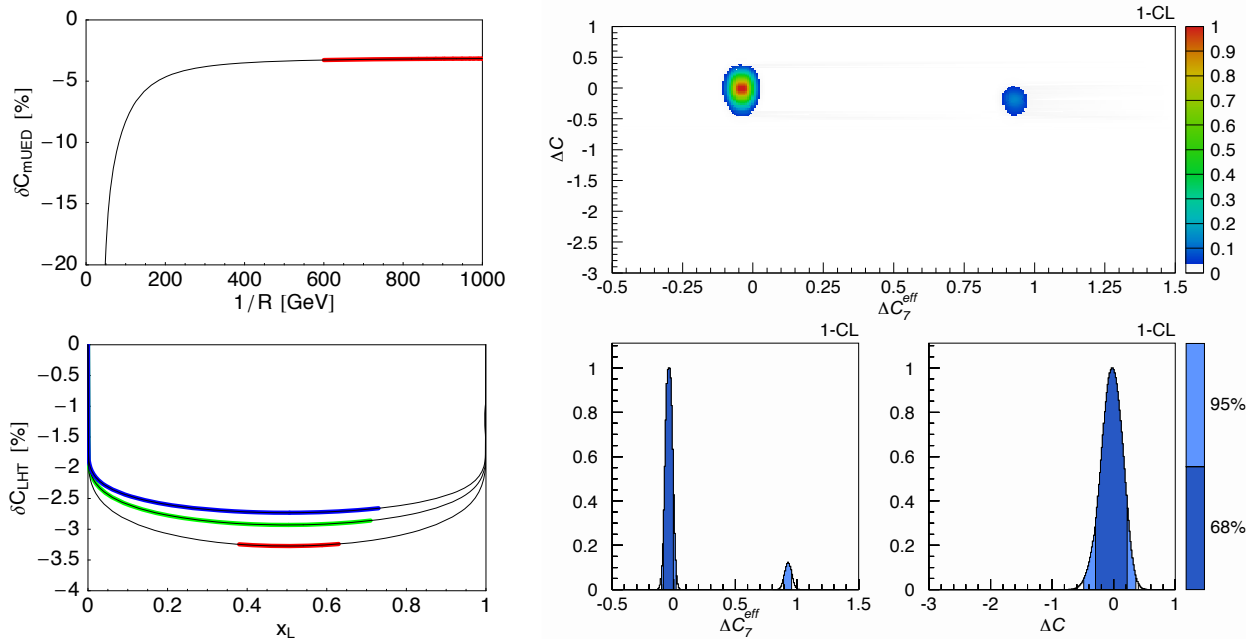


Figure 2: Left: Relative difference  $\delta C_{\text{BSM}}$  in the mUED and the LHT model as a function of  $1/R$  and  $x_L$ . In the case of the LHT model the shown curves correspond, from bottom to top, to the values  $f = 1, 1.5$ , and  $2 \text{ TeV}$  of the symmetry breaking scale. Right: Constraints on  $\Delta C_7^{\text{eff}}$  and  $\Delta C$  within CMFV that follow from a combination of the  $Z \rightarrow b\bar{b}$  pseudo observables with the measurements of  $\bar{B} \rightarrow X_s \gamma$  and  $\bar{B} \rightarrow X_s l^+ l^-$ . The colors encode the frequentist  $1 - \text{CL}$  level and the corresponding 68% and 95% probability regions as indicated by the bars on the right side of the panels. See text for details.

and  $\mathcal{B}(K^+ \rightarrow \pi^+ \nu \bar{\nu})$  does not allow to distinguish the SM solution  $\Delta C = 0$  from the wrong-sign case  $\Delta C \approx -2$ . The constraints on  $\Delta C$  within CMFV following from the simultaneous use of  $R_b^0$ ,  $\mathcal{A}_b$ ,  $A_{\text{FB}}^{0,b}$ ,  $\mathcal{B}(\bar{B} \rightarrow X_s \gamma)$ , and  $\mathcal{B}(\bar{B} \rightarrow X_s l^+ l^-)$  can be seen on the right-hand side of Fig. 2.

One can also infer from this figure that two regions, resembling the two possible signs of the amplitude  $\mathcal{A}(b \rightarrow s \gamma) \propto C_7^{\text{eff}}(m_b)$ , satisfy all existing experimental bounds. The best fit value for  $\Delta C_7^{\text{eff}} = C_7^{\text{eff}}(m_b) - C_{7\text{SM}}^{\text{eff}}(m_b)$  is very close to the SM point residing in the origin, while the wrong-sign solution located on the right is highly disfavored, as it corresponds to a  $\mathcal{B}(\bar{B} \rightarrow X_s l^+ l^-)$  value considerably higher than the measurements [14]. The corresponding limits are [6]

$$\Delta C_7^{\text{eff}} = -0.039 \pm 0.043 \quad (68\% \text{ CL}), \quad \Delta C_7^{\text{eff}} = [-0.104, 0.026] \cup [0.890, 0.968] \quad (95\% \text{ CL}). \quad (8)$$

Similar bounds have been presented previously in [13]. Notice that since the SM prediction of  $\mathcal{B}(\bar{B} \rightarrow X_s \gamma)$  [15] is now lower than the experimental world average by  $1.2\sigma$ , extensions of the SM that predict a suppression of the  $b \rightarrow s \gamma$  amplitude are strongly constrained. In particular, even the SM point  $\Delta C_7^{\text{eff}} = 0$  is almost disfavored at 68% CL by the global fit.

The stringent bound on the BSM contribution  $\Delta C$  given in Eq. (7) translates into tight two-sided limits for the branching ratios of all  $Z$ -penguin dominated flavor-changing  $K$ - and  $B$ -decays as shown in Tab. I. A strong violation of any of the bounds by future measurements will imply a failure of the CMFV hypothesis, signaling either the presence of new effective operators and/or new flavor and CP violation. A way to evade the given limits is the presence of sizable corrections  $\delta C_{\text{BSM}}$  and/or box contributions. While these possibilities cannot be fully excluded, general arguments and explicit calculations indicate that they are both difficult to realize in the CMFV framework.

Observable	CMFV (95% CL)	SM (68% CL)	SM (95% CL)	Experiment
$\mathcal{B}(K^+ \rightarrow \pi^+ \nu \bar{\nu}) \times 10^{11}$	[4.29, 10.72]	$7.15 \pm 1.28$	[5.40, 9.11]	$(17.3^{+11.5}_{-10.5})$ [16]
$\mathcal{B}(K_L \rightarrow \pi^0 \nu \bar{\nu}) \times 10^{11}$	[1.55, 4.38]	$2.79 \pm 0.31$	[2.21, 3.45]	$< 6.7 \times 10^3$ (90% CL) [17]
$\mathcal{B}(K_L \rightarrow \mu^+ \mu^-)_{\text{SD}} \times 10^9$	[0.30, 1.22]	$0.70 \pm 0.11$	[0.54, 0.88]	–
$\mathcal{B}(\bar{B} \rightarrow X_d \nu \bar{\nu}) \times 10^6$	[0.77, 2.00]	$1.34 \pm 0.05$	[1.24, 1.45]	–
$\mathcal{B}(\bar{B} \rightarrow X_s \nu \bar{\nu}) \times 10^5$	[1.88, 4.86]	$3.27 \pm 0.11$	[3.06, 3.48]	$< 64$ (90% CL) [18]
$\mathcal{B}(B_d \rightarrow \mu^+ \mu^-) \times 10^{10}$	[0.36, 2.03]	$1.06 \pm 0.16$	[0.87, 1.27]	$< 1.8 \times 10^2$ (95% CL) [19]
$\mathcal{B}(B_s \rightarrow \mu^+ \mu^-) \times 10^9$	[1.17, 6.67]	$3.51 \pm 0.50$	[2.92, 4.13]	$< 5.8 \times 10^1$ (95% CL) [19]

Table I: Bounds for various rare decays in CMFV models at 95% probability, the corresponding values in the SM at 68% and 95% CL, and the available experimental information. See text for details.

## 5. CONCLUSIONS

We have emphasized that large contributions to the universal Inami-Lim function  $C$  in constrained minimal flavor violation that would reverse the sign of the standard  $Z$ -penguin amplitude are excluded by the existing measurements of the  $Z \rightarrow b\bar{b}$  pseudo observables performed at LEP and SLC. This underscores the outstanding role of electroweak precision tests in guiding us toward the right theory and immediately raises the question: what else can flavor physics learn from the high-energy frontier?

## References

- [1] A. J. Buras *et al.*, Phys. Lett. B **500**, 161 (2001).
- [2] G. D’Ambrosio *et al.*, Nucl. Phys. B **645**, 155 (2002).
- [3] M. Blanke *et al.*, JHEP **0610**, 003 (2006).
- [4] S. Casagrande *et al.*, JHEP **0808**, 018 (2008).
- [5] L. Randall and R. Sundrum, Phys. Rev. Lett. **83**, 3370 (1999).
- [6] U. Haisch and A. Weiler, Phys. Rev. D **76**, 074027 (2007).
- [7] T. Appelquist, H. C. Cheng and B. A. Dobrescu, Phys. Rev. D **64**, 035002 (2001).
- [8] N. Arkani-Hamed *et al.*, JHEP **0207**, 034 (2002).
- [9] H. C. Cheng and I. Low, JHEP **0309**, 051 (2003) and **0408**, 061 (2004).
- [10] I. Low, JHEP **0410**, 067 (2004).
- [11] U. Haisch and A. Weiler, Phys. Rev. D **76**, 034014 (2007).
- [12] J. Hubisz *et al.*, JHEP **0601**, 135 (2006).
- [13] C. Bobeth *et al.*, Nucl. Phys. B **726**, 252 (2005).
- [14] P. Gambino, U. Haisch and M. Misiak, Phys. Rev. Lett. **94**, 061803 (2005).
- [15] M. Misiak *et al.*, Phys. Rev. Lett. **98**, 022002 (2007); M. Misiak and M. Steinhauser, Nucl. Phys. B **764**, 62 (2007).
- [16] A. V. Artamonov *et al.* [E949 Collaboration], 0808.2459 [hep-ex].
- [17] J. K. Ahn *et al.* [E391a Collaboration], Phys. Rev. Lett. **100**, 201802 (2008).
- [18] R. Barate *et al.* [ALEPH Collaboration], Eur. Phys. J. C **19**, 213 (2001).
- [19] T. Aaltonen *et al.* [CDF Collaboration], Phys. Rev. Lett. **100**, 101802 (2008).